PHYSICAL REVIEW E **79**, 030104(R) (2009)

Resonant activation through effective temperature oscillation in a Josephson tunnel junction

Cheng Pan, Xinsheng Tan, and Yang Yu*
Department of Physics and National Laboratory of Solid State Microstructures, Nanjing University, Nanjing 210093, China

Guozhu Sun, Ling Kang, Weiwei Xu, Jian Chen, and Peiheng Wu
Department of Electronic Science and Engineering, Research Institute of Superconductor Electronics, Nanjing University, Nanjing 210093, China

(Received 10 September 2008; published 23 March 2009)

We experimentally investigated the thermal escape from a metastable state in a Josephson tunnel junction subjected to an oscillating effective temperature. A minimum of the average escape time is observed at certain oscillation frequency. Our results confirm that the resonant activation can be caused not only by the oscillating barrier but also by the oscillating temperature. The linear dependence of the minimum average escape time on the resonant frequency suggests that the correlation between the oscillation and the escape process leads to the resonant escape.

DOI: 10.1103/PhysRevE.79.030104 PACS number(s): 05.40.−a, 02.50.−r, 74.50.+r

In the standard Kramers description of the thermal activation, the escape rate of a particle of mass m over a potential barrier ΔU at temperature T is given by the Arrhenius law [1]

$$\Gamma = \frac{a_t \omega_p}{2\pi} \exp(-\Delta U / k_B T), \tag{1}$$

where k_B is Boltzmann constant and $\omega_p/2\pi$ is the attempt frequency and usually identical to the natural frequency of the system. The prefactor a_t is weakly dependent on the damping of the system [1,2]. The barrier height ΔU and temperature T are important parameters dominating the escape rate since they are in the exponent. In addition, Eq. (1) is only valid for $\Delta U \gg k_B T$. Therefore Γ is usually investigated experimentally in the regime where Γ is several orders of magnitude smaller than ω_p.

If one applies a weak periodical driving force to the system, the synchronization of the escape and the driving period can induce some interesting resonant phenomena. One of those is the stochastic resonance [3–6], which has found important applications in nonlinear optics, solid-state devices, chemistry reactions, and neurophysiology. Another is the resonant activation [7–16], which shows that when potential barrier is fluctuating, a minimum of the average escape time ($\sim 1/\Gamma$) would occur at certain fluctuation rate. Since the resonant frequency is close to Γ, the resonant activation is totally different from the dynamic resonance that requires the driving frequency matching the natural frequency of the system [17,18]. It was found that the resonant activation is originated from the strong correlation between the potential fluctuations and the crossing time over barriers. Recently, Iwaniszewski and Wozinski [19] predicted that the resonant activation could also be caused by fluctuating temperature (FT). They pointed out that as potential barrier and temperature contribute to thermal escape rate in a similar way, fluctuating temperature and fluctuating barrier (FB) should lead to the same effect. In this Rapid Communication, we measured the thermal escape from a metastable state in a Josephson tunnel junction. The white noises with different values were applied to generate different effective temperatures on the junction. Then we can select two noise values and make the system oscillating between two effective temperatures. A minimum of average escape time is observed at a resonant frequency. Moreover, the resonant frequency is proportional to the average escape time. Our results confirm that the oscillating temperature can also lead to the resonant activation due to the correlation between the escape time and the temperature fluctuation.

A current-biased Josephson tunnel junction is an excellent system to study the thermal escape from a metastable state [20,21]. The equation of motion of a current-biased Josephson tunnel junction is identical to that of a particle moving in a washboard potential (Fig. 1) [20,22],

$$\frac{\hbar C}{2e}\frac{d^2\varphi}{dt^2} + \frac{\hbar}{2eR}\frac{d\varphi}{dt} + I_c \sin\varphi = I, \tag{2}$$

where φ is the phase difference across the junction and C, R, and I_c are the shunt capacitance, resistance, and the critical current of the junction, respectively. One can find that the mass of the particle is proportional to C and the damping of the system is proportional to $1/R$. When the bias current I is slightly smaller than I_c, the potential consists of a series of metastable wells with barrier height

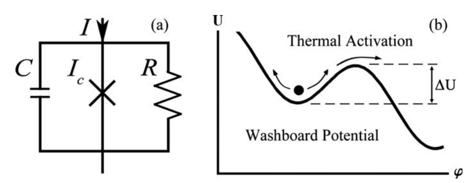

FIG. 1. (a) Equivalent circuit of a current-biased Josephson tunnel junction. (b) Washboard potential and the barrier height ΔU of a current-biased Josephson tunnel junction.

*yuyang@nju.edu.cn

$$\Delta U = 2E_J(\sqrt{1-i^2} - i\cos^{-1} i), \tag{3}$$

where $i=I/I_c$ is the normalized bias current and $E_J=I_c\frac{\hbar}{2e}$ is the Josephson energy. A particle, which is initially trapped in a well (corresponding to a zero-voltage state), can be activated out of it by thermal fluctuation and then the junction switches to a finite-voltage state [18,23]. With the thermal fluctuation, the junction switching to the voltage state is a deterministic random process. The switching current distribution $P(I)$ is given by [23,24]

$$P(I) = \frac{\Gamma(I)}{dI/dt}\exp\left[-\frac{1}{dI/dt}\int_0^I \Gamma(I')dI'\right], \tag{4}$$

where $\Gamma(I)$ is the escape rate corresponding to the bias current I and dI/dt stands for the ramp rate of the bias current during the measurement. For a current-biased Josephson junction the parameters in Eqs. (1) and (4) are well controllable and one can extract useful information of the system by measuring $P(I)$ [23,25].

At finite environmental temperature, there is a thermal noise current generated by R to the system and Eq. (2) can be rewritten in the form [23,24]

$$\frac{\hbar C}{2e}\frac{d^2\varphi}{dt^2} + \frac{\hbar}{2eR}\frac{d\varphi}{dt} + I_c \sin\varphi = I + I_n(t). \tag{5}$$

The thermal noise is in form of the white Gaussian noise and the current $I_n(t)$ is related with temperature T as

$$\langle I_n(t)I_n(t')\rangle = 2\frac{k_BT}{R}\delta(t-t'). \tag{6}$$

If we apply an additional white noise current $I_n'(t)$ to a current-biased junction, the total noise current $I_{\rm ns}(t)$ defined an effective temperature,

$$\langle I_{\rm ns}(t)I_{\rm ns}(t')\rangle = 2\frac{k_BT_{\rm eff}}{R}\delta(t-t'), \tag{7}$$

where the effective temperature $T_{\rm eff}=T+RI_\sigma^2/2k_B$ and I_σ is the rms of the white Gaussian noise $\langle I_n'(t)I_n'(t')\rangle=I_\sigma^2\delta(t-t')$. Therefore $T_{\rm eff}$ can be adjusted by tuning I_σ, which is proportional to $V_{\rm rms}$ of the noise source. Furthermore, the effective temperature of the junction can be verified independently by measuring the switching current distribution. Figure 2 shows the measured $P(I)$ with different I_σ's of the white noise current. With I_σ increasing, the mean of the switching current distribution shifts to lower value and the width of the distribution increases. This behavior of the switching distribution is identical to that of increasing the bath temperature. Using Eqs. (1) and (4), we can fit $P(I)$ to obtain an effective temperature quantitatively. The good linear relation between $T_{\rm eff}$ and T_σ [inset (B) of Fig. 2] indicates that we successfully changed the effective temperature of the system by tuning I_σ. This provides us a convenient method to realize an oscillating effective temperature in a Josephson tunnel junction, which is otherwise difficult to produce because of the large thermal mass of the sample holder.

The sample used in this study is a NbN/AlN/NbN Josephson tunnel junction which has critical temperature $T_c\approx 16$ K. The size of the junction is 10×10 μm^2. The

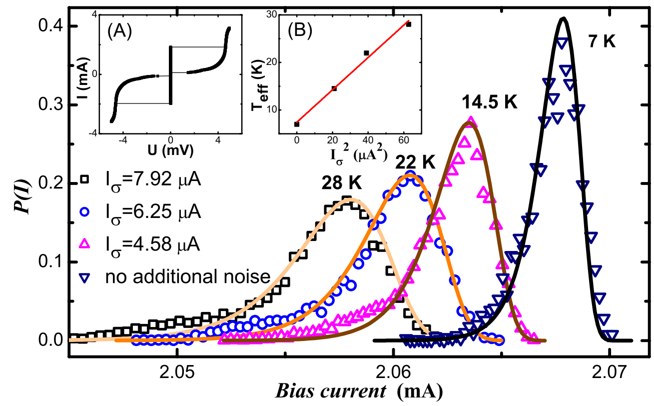

FIG. 2. (Color online) The switching current distribution of the junction with various values of additional white noise current. Solid lines are calculated distributions with effective temperatures of 28, 22, 14.5, and 7 K, respectively. Inset (A): *I-V* curve of the NbN/AlN/NbN sample used in our experiment. Inset (B): effective temperature as a function of I_σ^2. The solid line is the best fit.

critical current and the capacitance of the junction are $I_c\approx 2.1$ mA and $C\approx 5$ pF, respectively. The normal-state resistance of the junction is $R_n\sim 2$ Ω, resulting a quality factor of $Q\equiv\omega_{p0}R_nC=\sqrt{\frac{2eI_c}{\hbar C}}R_nC\approx 11$. Therefore the system is underdamped and a large hysteresis was observed in the *I-V* characteristic [inset (A) of Fig. 2]. The sample is mounted on a chip carrier within a copper cell which is then dipped into liquid helium. We filled the copper cell with helium as the heat exchange gas to keep the sample in thermal equilibrium. Twisted wires with 1 kΩ resistor at 4.2 K were used to connect the junction to the room-temperature circuitry. The bandwidth of the measurement system is about 100 kHz. The escape rate investigated here is in the range of kHz. Therefore, we can consider that the additional white noise, which is generated by a signal generator, only increases the effective temperature. We first calibrated the experimental setup by measuring the switching distribution. A sawtooth bias current was applied with a repetition rate of about 71 Hz. The current at which the junction switches from the zero-voltage state to finite-voltage state was recorded. By making the histogram of the switching current, we obtained the switching current distribution shown in Fig. 2. The agreement between the theory and the experimental results is remarkable. We noticed that for $I_\sigma=0$, the effective temperature is about 7 K, which is higher than the bath temperature

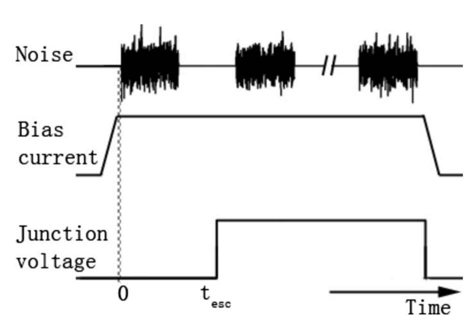

FIG. 3. Schematic time profile for measuring the escape time of a Josephson junction with presence of an oscillating white noise.

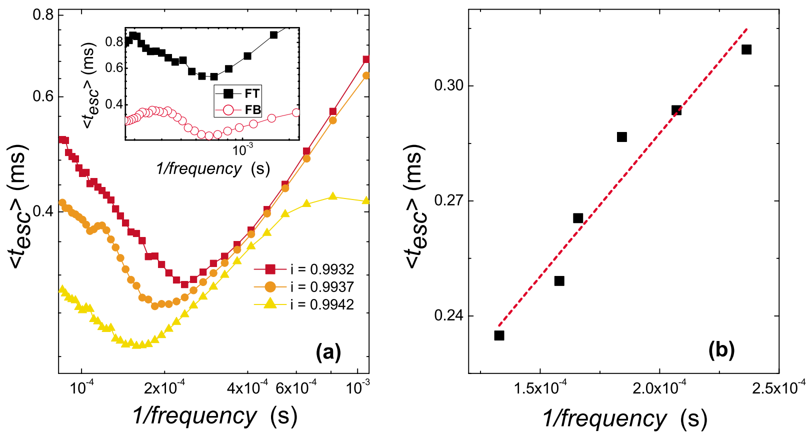

FIG. 4. (Color online) (a) Average escape time $\langle t_{\mathrm{esc}}\rangle$ as a function of characteristic time of temperature fluctuation $1/f$ for different I's. The currents normalized to I_c were shown in the right corner. The two values of the oscillating noise are $I_\sigma=0$ and 4.17 μA, respectively. The valleys of the curves indicate the resonant activation with the resonant frequency depending on the bias current. Inset: $\langle t_{\mathrm{esc}}\rangle$ as a function of the characteristic time of barrier fluctuation for FB. (b) Minimum average escape time (or maximum escape rate) as a function of inverted resonant frequency $1/f_{\mathrm{res}}$. The dashed line is the best fit with a slope of 0.74 ± 0.08.

of 4.2 K. Since no substantial peak at 50 Hz and its harmonics were found on the junction voltage noise spectrum, a reasonable explanation for the high base temperature is the heating effect due to the large critical current density (~ 2 kA/cm^2) and high gap voltage (~ 5 mV) of the junction. It is worth to emphasize that the high base temperature will not affect our results as long as the sample is in the thermal equilibrium.

In order to investigate the resonant escape, we measured the escape time of the junction using time-of-flight method [26,27]. We started each cycle by ramping up the bias current to I, which results a washboard potential well with barrier height of ΔU according to Eq. (3), and maintained at this level for a period of waiting time. During the waiting time, we added a white noise current i_n periodically with frequency f to make the system fluctuating between two effective temperatures, as shown in Fig. 3. For the zero I_σ, the effective temperature is at a low value T_l. For the finite I_σ, the effective temperature corresponds to a high value T_h. It is worth to mention that $2\pi f \ll \omega_p$; therefore, the dynamic resonant escape from the system cannot happen [17,18]. Once the junction escapes from the potential well, the voltage jumps from zero to finite and this signal was used to stop the timer. The duration of this waiting period was recorded then we decreased the bias current and initialized the system again. After repeating this process more than 10^3 times, we obtained an average escape time $\langle t_{\mathrm{esc}}\rangle$. We observed a nonmonotonic behavior by plotting $\langle t_{\mathrm{esc}}\rangle$ as a function of $1/f$ (Fig. 4), which stands for the characteristic time of temperature fluctuation. Although our junction is an underdamped system, the resonant activation exhibits the main feature predicted by Iwaniszewski and Wozinski [19]. $\langle t_{\mathrm{esc}}\rangle$ at slow fluctuation rate is always larger than that at fast fluctuation rate. For comparison, we also add sinusoidal current to the bias current instead of white noise to produce the FB-caused resonant activation. As expected the resonance at similar frequency was observed [inset of Fig. 4(a)]. We defined the resonant frequency f_{res} where $\langle t_{\mathrm{esc}}\rangle$ is a minima; it is found that f_{res} increased with the bias current. Since the higher the bias current the larger the escape rate, it is evident that the resonant activation is caused by the correlation between the barrier crossing and the temperature oscillation. This argument was confirmed by the good linear relation between $\langle t_{\mathrm{esc}}\rangle$ and the resonant frequency [Fig. 4(b)].

The FT-caused resonant activation can also be tuned if we keep the bias current unchanged and modulate I_σ to change T_h. Shown in Fig. 5(a) are some examples of $\langle t_{\mathrm{esc}}\rangle$ vs $1/f$. As the effective temperature difference $T_h - T_l$ increases, the valley of the curve becomes deeper and narrower. Furthermore, the minimum moves to higher frequency. Figure 5(b) shows that the minimum of $\langle t_{\mathrm{esc}}\rangle$ increases linearly with the inverse resonant frequency. This is consistent with the previous results and discussion.

From Figs. 4(b) and 5(b) we have $\langle t_{\mathrm{esc}}\rangle f_{\mathrm{res}} \approx 0.70$. This value is about the same with that of the FB-caused resonant activation. However, previous works on the underdamped

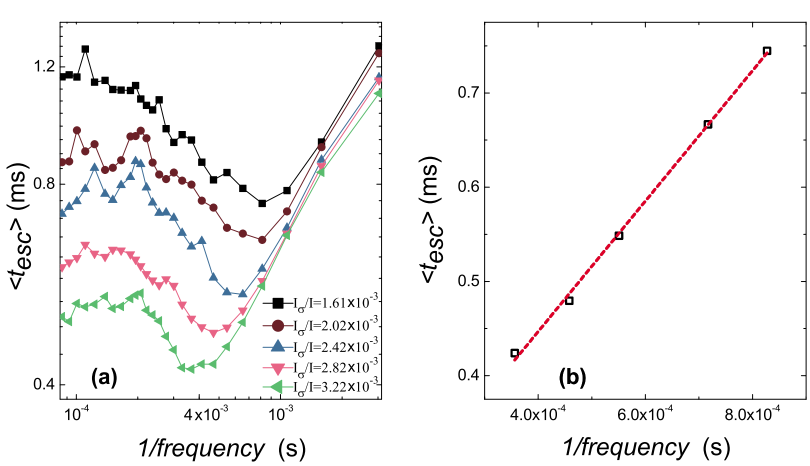

FIG. 5. (Color online) (a) $\langle t_{\mathrm{esc}}\rangle$ vs $1/f$ for various I_σ's (normalized to I). The minimums on $\langle t_{\mathrm{esc}}\rangle$ indicate the presence of the resonant activation. (b) Minimum $\langle t_{\mathrm{esc}}\rangle$ vs resonant $1/f$. The dashed line is the best fit with a slope of 0.70 ± 0.02.

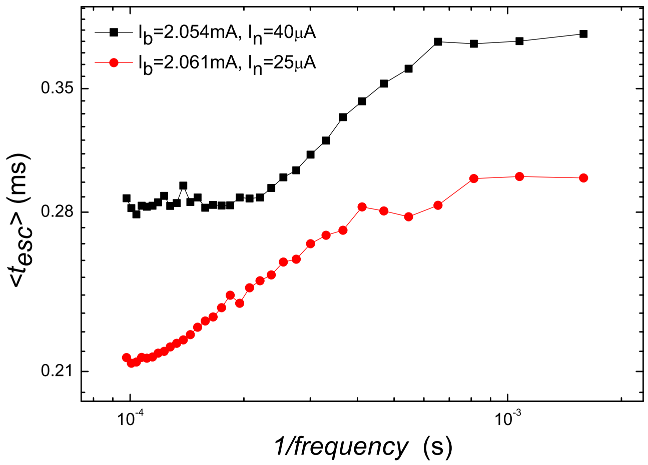

FIG. 6. (Color online) Resonant activation disappears when $\Delta U/k_BT<1$. Solid squares above show the measured $\langle t_{\text{esc}}\rangle$ as a function of $1/f$ at relatively large I_σ. Solid circles are $\langle t_{\text{esc}}\rangle$ vs $1/f$ at a relatively large I which corresponds to a lower ΔU. In both cases $\Delta U/k_BT$ is reduced and the resonant activation disappears as predicted.

Josephson junctions reported $\langle t_{\text{esc}}\rangle f_{\text{res}}\approx 0.25$ [15,16]. This indicates that $\langle t_{\text{esc}}\rangle f_{\text{res}}$ is dependent on the system.

Another important prediction is that when $\Delta U/k_BT<1$, the FT-caused resonant activation will disappear [19] because Eq. (1) is not valid and the system enters a diffusion transition in this regime [28–31]. We confirmed this by increasing the bias current or the noise current I_σ, corresponding to lowering the barrier or increasing the effective temperature. Figure 6 shows measured $\langle t_{\text{esc}}\rangle$ as a function of $1/f$ at large bias current and I_σ. Monotonic behavior is evident. This result suggested that we did raise the effective temperature by increasing I_σ.

In summary, we experimentally observed the resonant activation caused by oscillating temperature in an underdamped Josephson tunnel junction. Additional white noise current was applied in order to produce an environment of higher effective temperature. We investigated the thermal escape under an oscillating effective temperature. Resonant activation actually occurs when the temperature oscillation frequency matches the average escape time. The linear relation of the minimum average escape time and the resonant frequency suggests that the correlation between the oscillation and the escape process leads to the resonant escape.

We would like to thank S. Han for helpful discussion and technical support. This work was partially supported by NSFC (Contracts No. 10674062 and No. 10725415), the State Key Program for Basic Research of China (Contract No. 2006CB921801), and the Doctoral Funds of Ministry of Education of the People's Republic of China (Contract No. 20060284022).

[1] P. Hänggi, P. Talkner, and M. Borkovec, Rev. Mod. Phys. **62**, 251 (1990).
[2] M. Büttiker, E. P. Harris, and R. Landauer, Phys. Rev. B **28**, 1268 (1983).
[3] S. Fauve and F. Heslot, Phys. Lett. **97A**, 5 (1983).
[4] B. McNamara, K. Wiesenfeld, and R. Roy, Phys. Rev. Lett. **60**, 2626 (1988).
[5] L. Gammaitoni, P. Hänggi, P. Jung, and F. Marchesoni, Rev. Mod. Phys. **70**, 223 (1998).
[6] M. I. Dykman, D. G. Luchinsky, P. V. E. McClintock, N. D. Stein, and N. G. Stocks, Phys. Rev. A **46**, R1713 (1992).
[7] C. R. Doering and J. C. Gadoua, Phys. Rev. Lett. **69**, 2318 (1992).
[8] M. Marchi, F. Marchesoni, L. Gammaitoni, E. Menichella-Saetta, and S. S. Santucci, Phys. Rev. E **54**, 3479 (1996).
[9] J. Iwaniszewski, Phys. Rev. E **54**, 3173 (1996).
[10] B. Spagnolo, A. A. Dubkov, A. L. Pankratov, E. V. Pankratova, A. Fiasconaro, and A. Ochab-Marcinek, Acta Phys. Pol. B **38**, 1925 (2007).
[11] U. Zürcher and C. R. Doering, Phys. Rev. E **47**, 3862 (1993).
[12] M. Bier and R. D. Astumian, Phys. Rev. Lett. **71**, 1649 (1993).
[13] P. Pechukas and P. Hänggi, Phys. Rev. Lett. **73**, 2772 (1994).
[14] R. N. Mantegna and B. Spagnolo, Phys. Rev. Lett. **84**, 3025 (2000).
[15] G. Sun *et al.*, Phys. Rev. E **75**, 021107 (2007).
[16] Y. Yu and S. Han, Phys. Rev. Lett. **91**, 127003 (2003).
[17] M. H. Devoret, J. M. Martinis, D. Esteve, and J. Clarke, Phys. Rev. Lett. **53**, 1260 (1984).
[18] J. M. Martinis, M. H. Devoret, and J. Clarke, Phys. Rev. B **35**, 4682 (1987).
[19] J. Iwaniszewski and A. Wozinski, EPL **82**, 50004 (2008).
[20] W. C. Stewart, Appl. Phys. Lett. **12**, 277 (1968).
[21] D. E. McCumber, J. Appl. Phys. **39**, 3113 (1968).
[22] A. Barone and G. Paterno, *Physics and Applications of the Josephson Effect* (Wiley, New York, 1982).
[23] T. A. Fulton and L. N. Dunkleberger, Phys. Rev. B **9**, 4760 (1974).
[24] A. Barone, R. Cristiano, and P. Silvestrini, J. Appl. Phys. **58**, 3822 (1985).
[25] S.-X. Li *et al.*, Phys. Rev. Lett. **89**, 098301 (2002).
[26] S. Han *et al.*, Science **293**, 1457 (2001).
[27] Y. Yu *et al.*, Supercond. Sci. Technol. **15**, 555 (2002).
[28] J. M. Martinis and R. L. Kautz, Phys. Rev. Lett. **63**, 1507 (1989).
[29] M. Iansiti, M. Tinkham, A. T. Johnson, W. F. Smith, and C. J. Lobb, Phys. Rev. B **39**, 6465 (1989).
[30] D. Vion, M. Götz, P. Joyez, D. Esteve, and M. H. Devoret, Phys. Rev. Lett. **77**, 3435 (1996).
[31] Y. Koval, M. V. Fistul, and A. V. Ustinov, Phys. Rev. Lett. **93**, 087004 (2004).